# CHAPTER IV

## RESULTS AND DISCUSSION

### 4.1 Synthesis of S-Benzoyl-mercaptoacetylglycylglycylglycine

#### 4.1.1 Preparation of S-Benzoylthioglycolic acid (I)

The thioesterification reaction for synthesis of S-Benzoylthioglycolic acid is shown below.

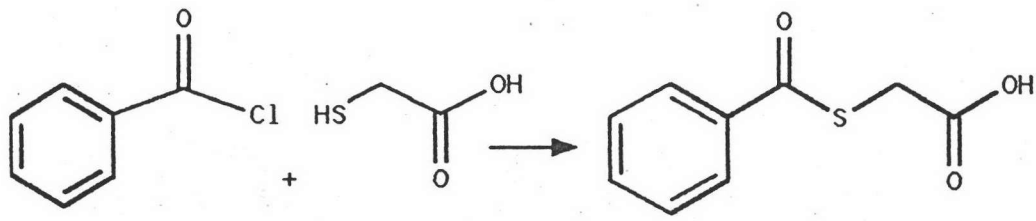


Benzoylchloride was introduced to react with thioglycolic acid in the mixture of toluene and alkali solution. Temperature of the reaction must be controlled at 10°C for 60 minutes. The mixture was left at room temperature (25°C) for 10 minutes until pink color occurred. The pure S-Benzoylthioglycolic acid of 70% yield was obtained as colouless crystal after acidification of the aqueous layer and recrystallization by ethylacetate.

4.1.2 Preparation of Succinimidyl-s-benzoyl thioglycolate

The dehydration reaction of succinimidyl active ester was obtained by s-benzoylthioglycolic acid and N-hydroxysuccinimide with dicyclohexylcarbodiimide as a dehydrating agent at -5°C in tetrahydrofuran. The reaction yielded are succinimidyl-s-benzoylthioglycolate and dicyclohexyl urea. The reaction is shown below .

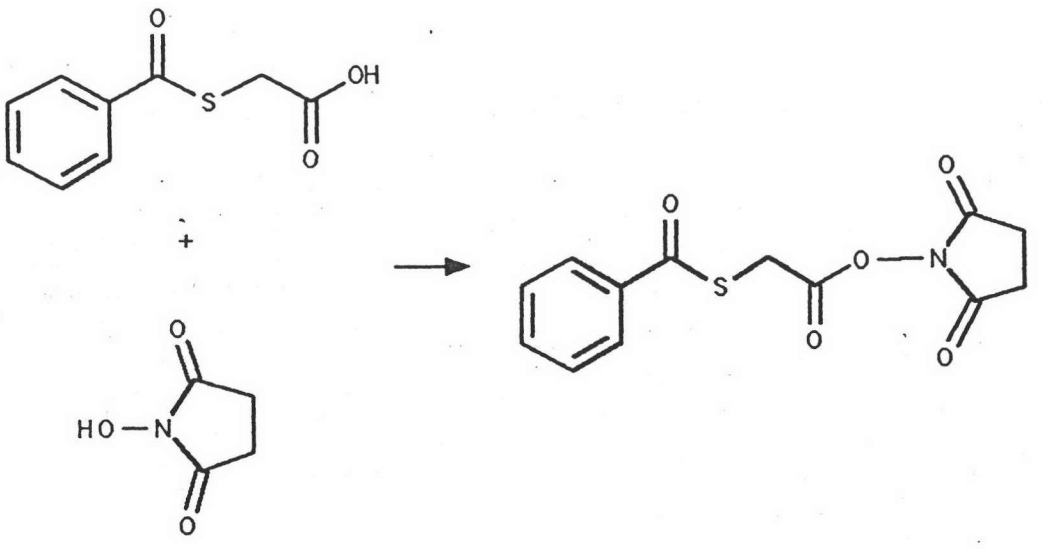

The dehydrating temperature was most important factor in this step .It must be kept at -5 ± 1 °C. The succinimidyl-s-benzoylthioglycolate was obtained as colorless needle crystal after recrystallization by ethylacetate with a yield 75.15% .

4.1.3 Preparation of S-Benzoylmercaptoacetylglycylglycylglycine (S-Bz-$MAG_3$)

The S-Bz-$MAG_3$ was synthesized from substitution reaction of amine ester by polypeptide (triglycine) in mild alkali media as shown below.

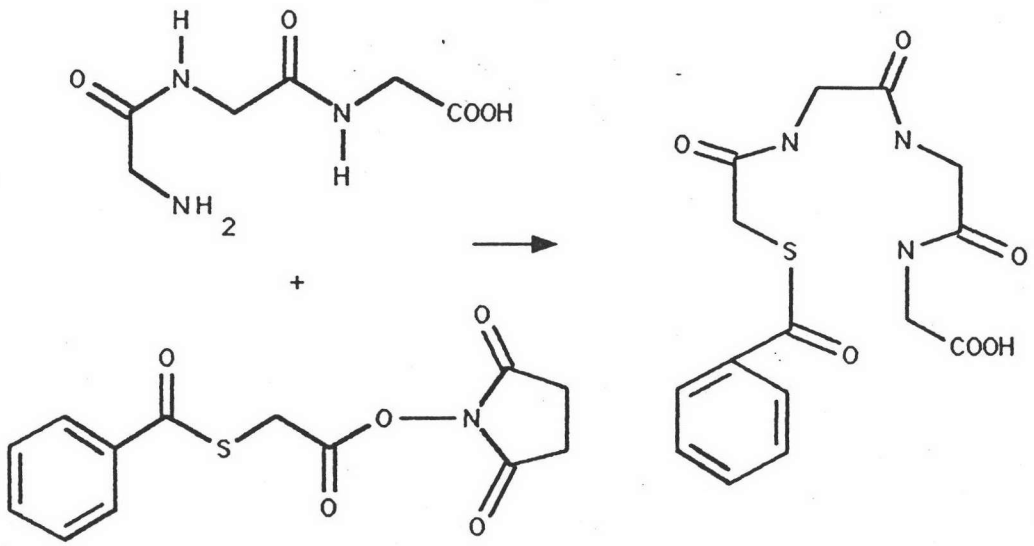

The reaction condition was mild and required a long period of time for substitution. In strong alkali media and high temperature, the product is decomposed to yellow solution and the yield is lower than 5%. This is probably due to possibility of benzoyl group lost. In order to obtain the good yield, 20 ml of 0.05 M. NaOH and 95% ethanol were used as solvent for dissolving triglycine and succinimidyl-s-thioglycolate respectively. The yield obtained from this reaction condition was 67.27% .

All physical properties of synthetic compound are listed in table 4.1

Table 4.1 Physical properties of the synthetic compounds.

| compound | m.p. °C | yield % | % composition (w/w) | | | |
|---|---|---|---|---|---|---|
| | | | %C | | %H | |
| | | | cal | Exp | cal | Exp |
| (I) | 104-105 | 70.1 | 55.09 | 56.84 ±0.07 | 4.11 | 4.13 ±0.01 |
| (II) | 135-136 | 75.75 | 53.24 | 52.62 ±0.03 | 3.78 | 3.32 ±0.04 |
| (III) | 193-195 | 67.27 | 48.65 | 49.18 ±0.03 | 5.13 | 5.30 ±0.02 |

(I) is S-Benzoylthioglycolic acid

(II) is Succinimidyl-S-Benzoylthioglycolate

(III) is S-Benzoyl-mercaptoacetylglycylglycylglycine

The synthesized compound were characterized by IR, NMR technique. The spectra and corresponding assignments of various synthesis products are shown in figure and table below.

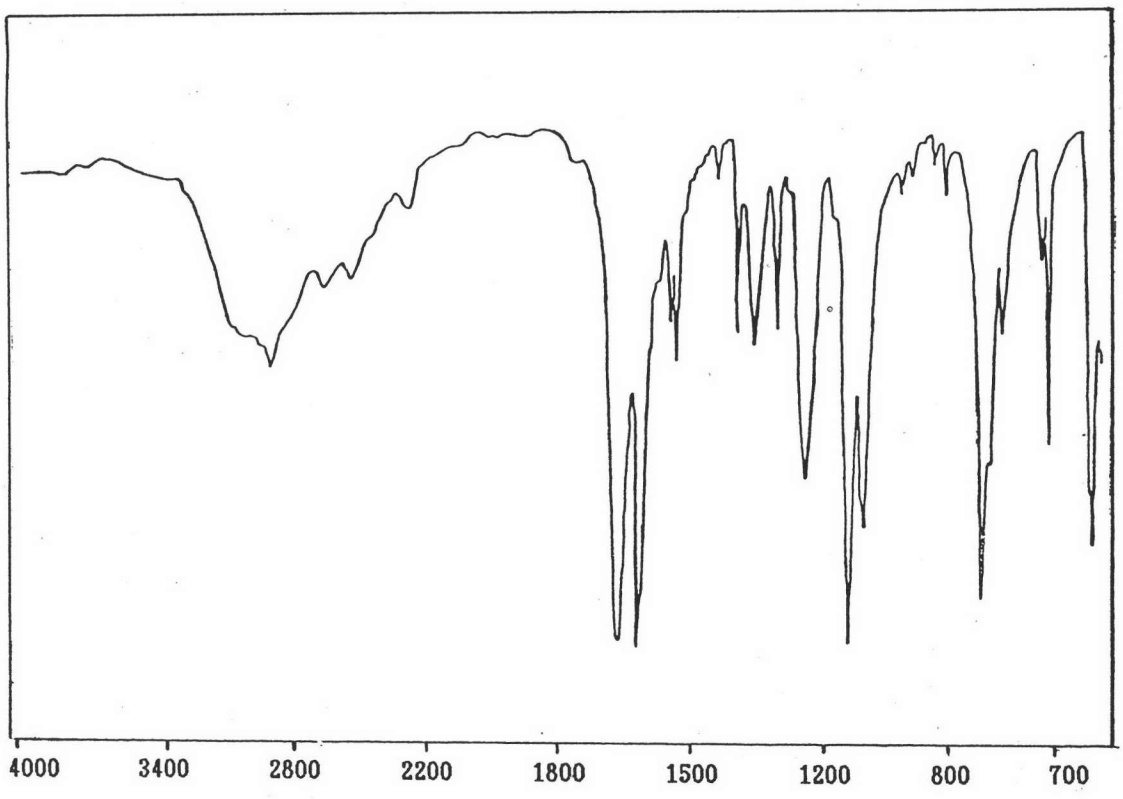


Figure 4.1 IR spectrum of S-Benzoythioglycolic acid (KBr)

Table 4.2 Wave number of S-Benzoylthioglycolic acid

| Absorption Frequency KBr, ($cm^{-1}$) | assignments |
|---|---|
| 2910 | - OH stretching |
| 1700 | -COOH stretching |
| 1660 | SC=O stretching |
| 1580,1600 | C=C stretching |
| 1410 | - OH inplane bending |
| 1700 | - OH out of plane bending |
| 680,775 | C-H out of plane bending |

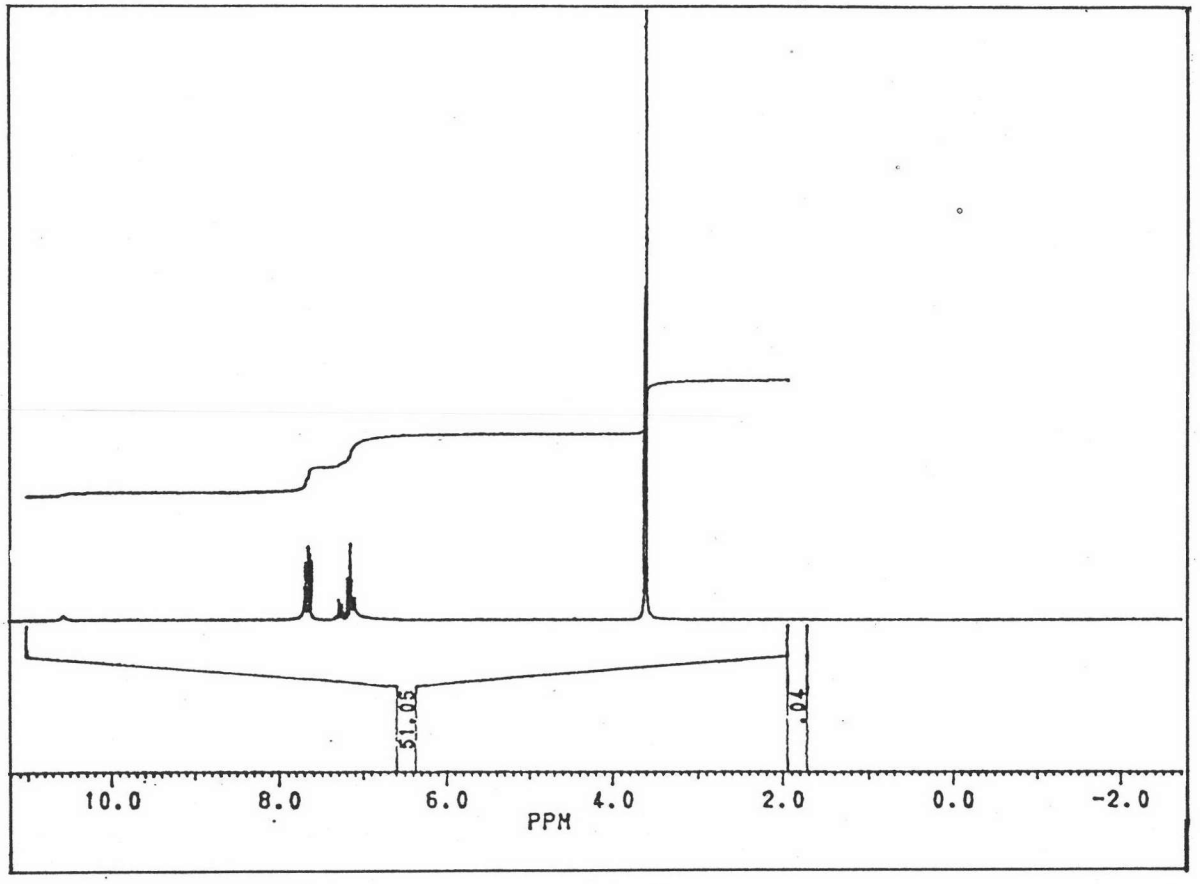


Figure 4.2 $H^1$-NMR spectrum of S-Benzoylthioglycolic acid

Table 4.3 $H^1$-Chemical Shift of S-Benzoylthioglycolic acid

| Chemical Shift ($CD_3Cl$ with TMS),(ppm) | assignments |
|---|---|
| 3.8 - 4.Ø5 | singlet, 2H,-S-$CH_2$-COOH |
| 7.2 - 8.7 | multiplet, 5H, Ar-H |

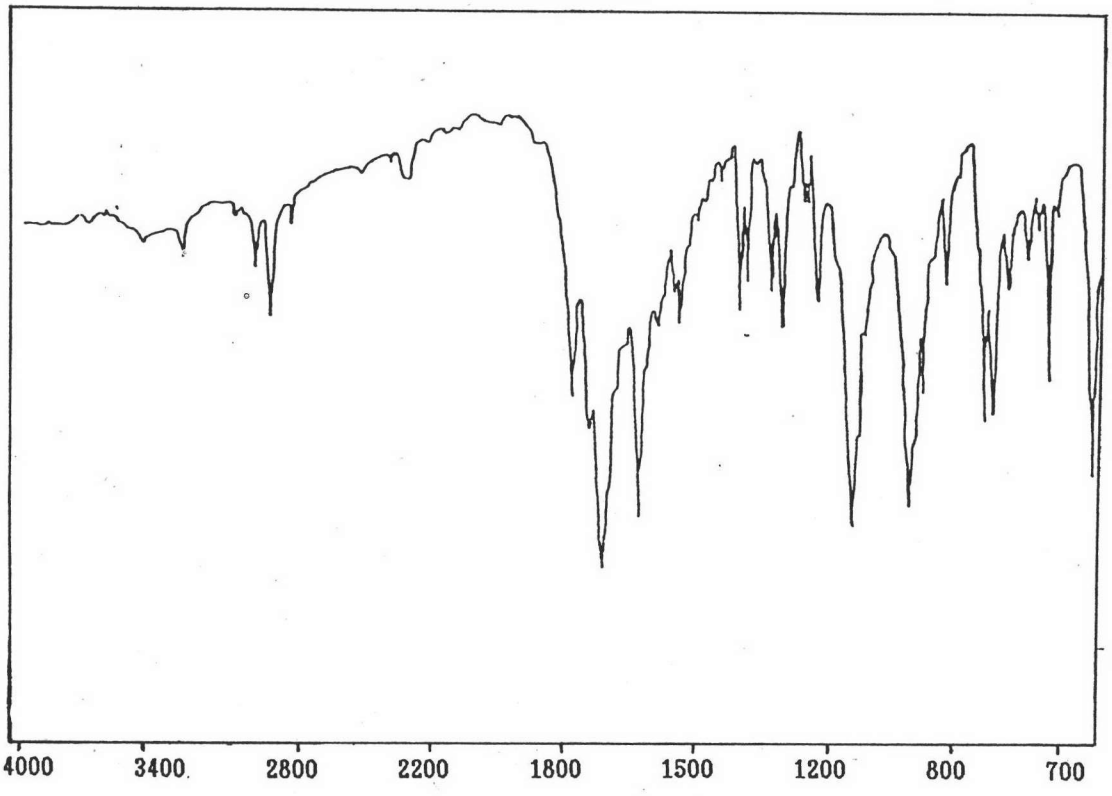


Figure 4.3 IR spectrum of Succinimidyl-S-Benzoylthiogly -colate (KBr)

Table 4.4 Wave number of Succinimidyl-S-Benzoylthio glycolate (KBr)

| Absorption Frequency KBr, ($cm^{-1}$) | assignments |
|---|---|
| 1810,1775,1740 | C=O stretching |
| 1665 | -S-C=O stretching |
| 1200 | N-O stretching |
| 680,.775 | C-H out of plane bending of monosubstituted benzene |

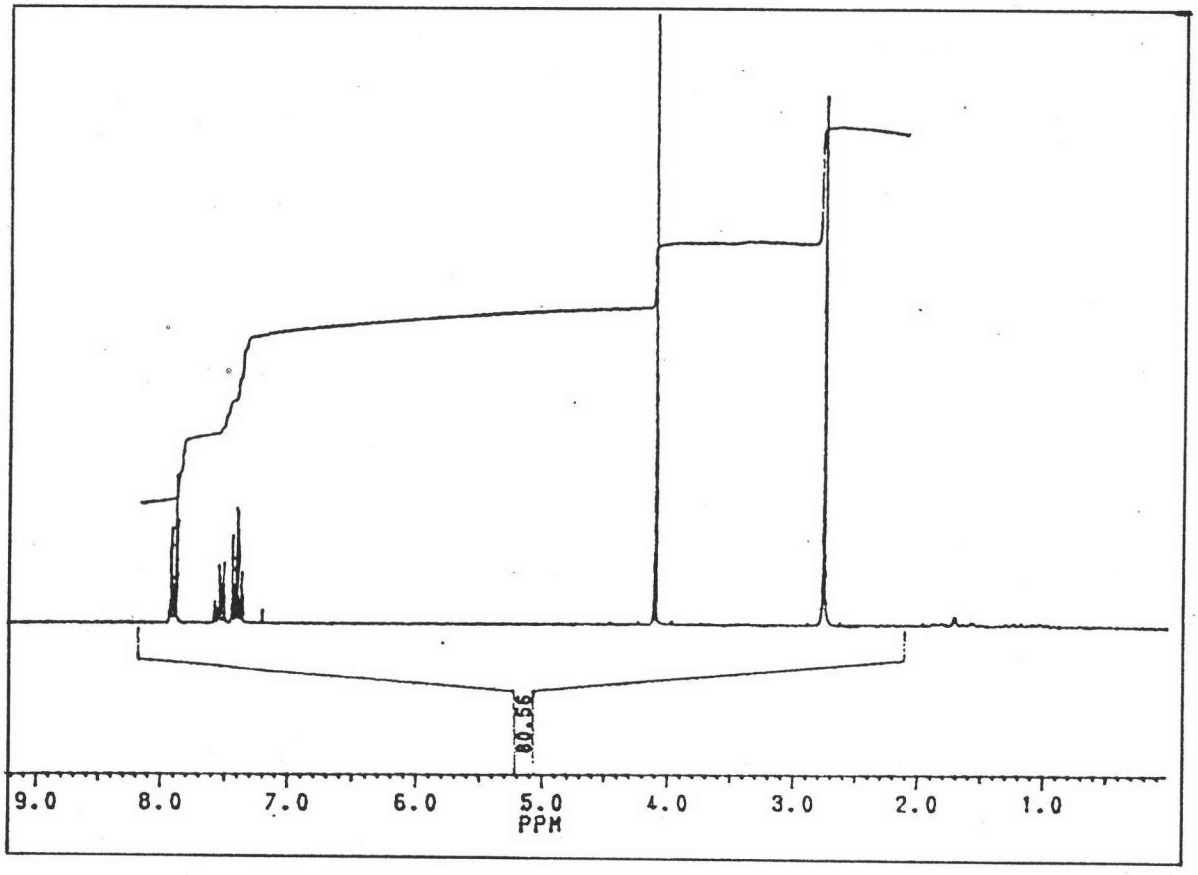


Figure 4.4 $H^1$-NMR spectrum of Succinimidyl-S-Benzoyl -thioglycolate

Table 4.5 $H^1$-Chemical Shift of Succinimidyl-S-Benzoyl -thioglycolate

| Chemical Shift ($CD_3Cl$ with TMS) (ppm) | assignments |
|---|---|
| 2.7 - 2.9 | singlet, 4H, $-CO-CH_2-CH_2-CO$ |
| 4.1 - 4.2 | singlet, 2H, $-S-CH_2-COO-$ |
| 7.3 - 8.05 | multiplet, 5H, Ar-H |

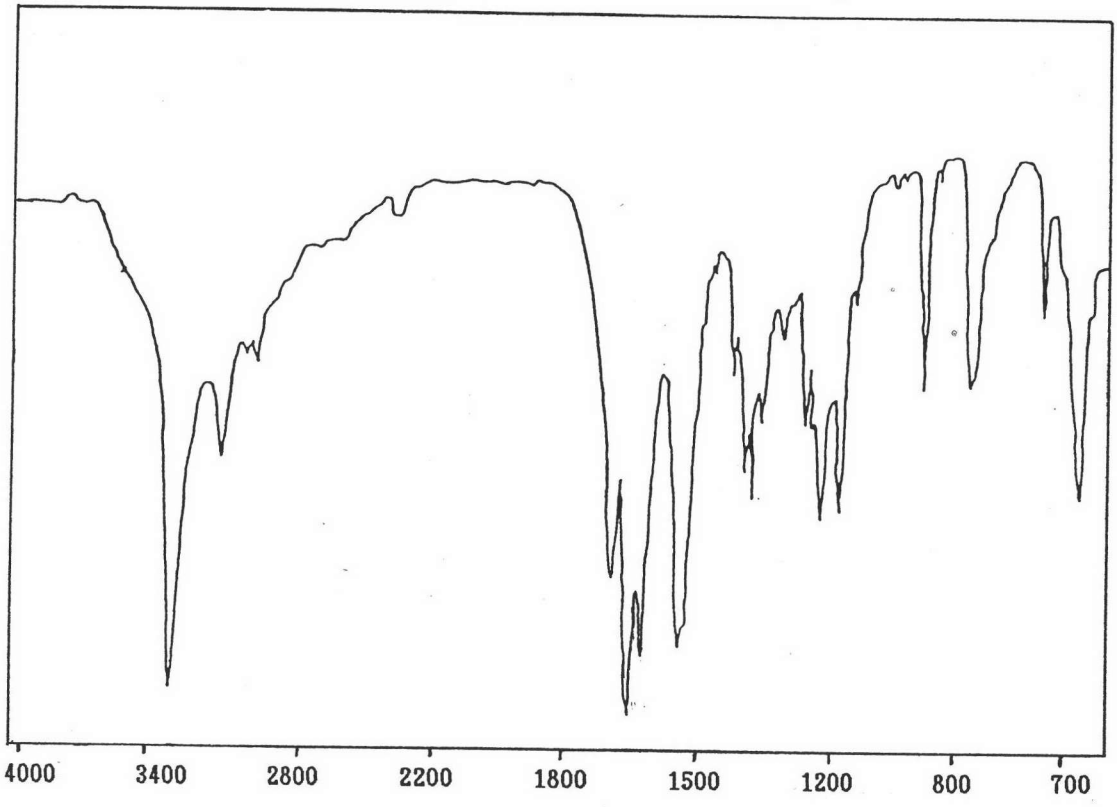


Figure 4.5 IR spectrum of S-Benzoyl-mercaptoacetylglycyl glycylglycine

Table 4.6 Wave number of S-Benzoyl-mercaptoacetylglycyl glycylglycine

| Absorption Frequency KBr, ($cm^{-1}$) | assignments |
|---|---|
| 3300,3070 | N-H stretching |
| 1700 | -COOH stretching |
| 1650 | -C-N stretching |
| 1635 | -S-C=O stretching |
| 1550 | N-H bending |
| 680,775 | C-H out of plane bending of monosubstituted benzene |

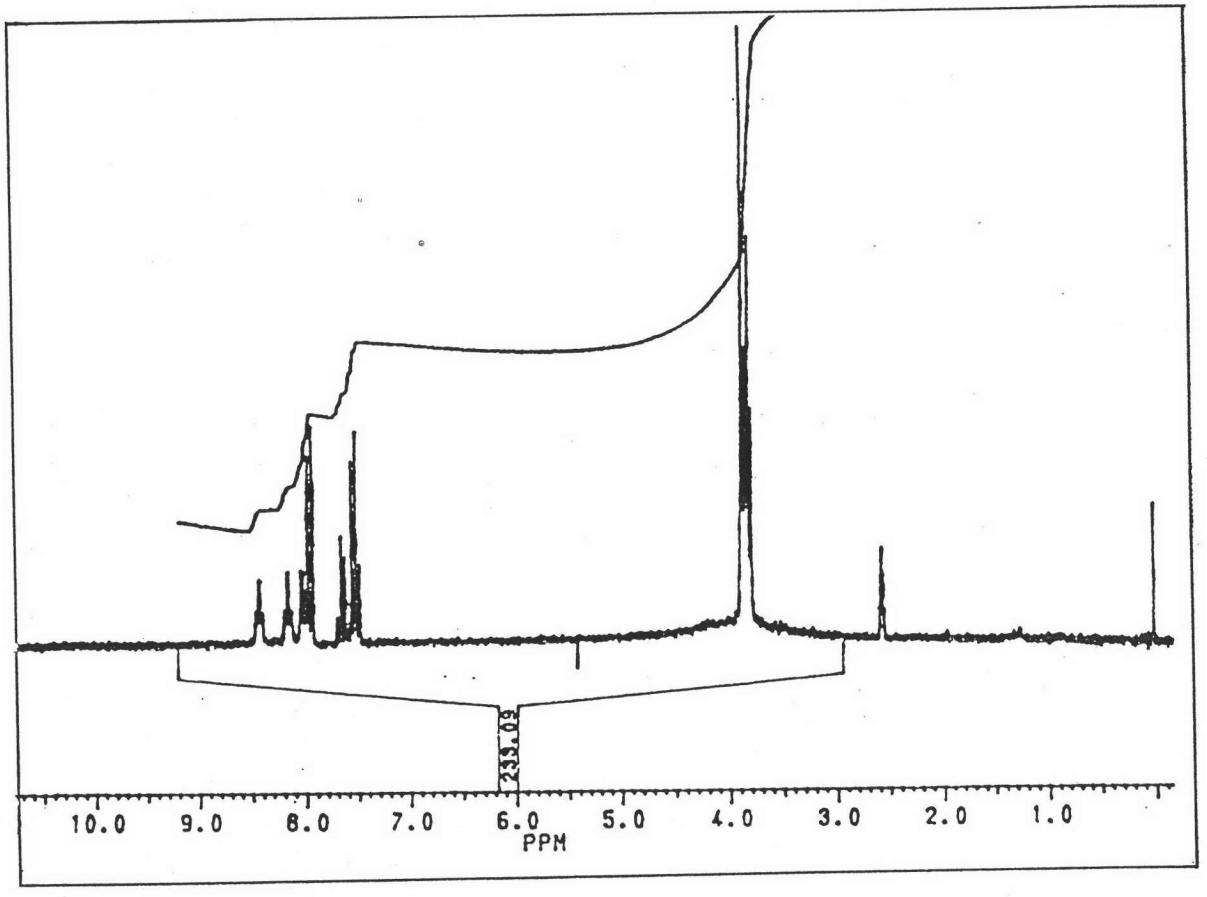


Figure 4.6 $H^1$-NMR spectrum of S-Benzoyl-mercaptoacetyl glycylglycylglycine

Table 4.7 $H^1$-Chemical Shift of S-Benzoyl-S-mercaptoacetyl glycylglycylglycine

| Chemical Shift ($CD_3Cl$ with TMS), (ppm) | assignments |
|---|---|
| 3.72- 3.79 | multiplet, 6H, 3, -N-$CH_2$-CO- |
| 3.89 | singlet, 2H, -S-$CH_2$-CO |
| 7.55 - 7.79 | multiplet, 5H, Ar-H |

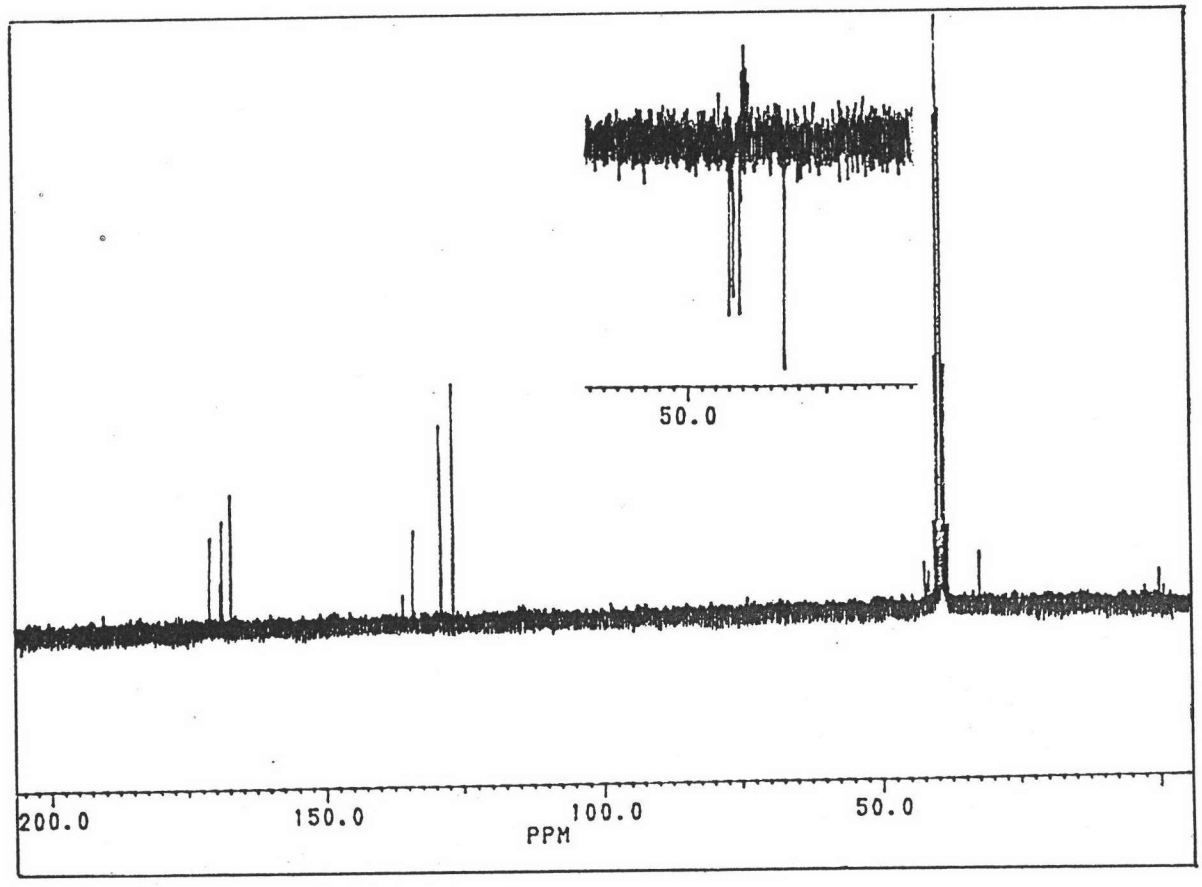


Figure 4.7 $C^{13}$-NMR spectrum of S-Benzoyl-mercaptoacetyl glycylglycylglycine in DMSO-$\alpha_6$

Table 4.7 $C^{13}$ Chemical Shift of S-Benzoyl-mercaptoacetyl glycylglycylglycine

| Chemical Shift ( DMSO $d_6$ ), (ppm) | assignments |
|---|---|
| 32.33 | $CH_2$ - S |
| 40.43, 40.65, 41.62 | $CH_2$ - N |
| 126.78, 129.07, 133.99 | -CH- (monosubstituted benzene) |
| 167.09, 168.75, 170.92 | C=O (amide) |
| 39.40 | DMSO - $d_6$ (multiplet) |

4.2 The preliminary preparation of $^{99m}Tc$-$MAG_3$ and determination of suitable separation method.

A kit, containing sodiumgluconate, S-Bz-$MAG_3$ and stannous chloride dihydrate as reducing agent was prepared by following Firtzberg's procedure (1986). By this method, the kit consists of 1 mg of S-Bz-$MAG_3$, 20 mg of sodium gluconate and 20 µg of stannous chloride dihydrate. After complexing with 25 mCi of pertechnetate ion, only one species is found (free pertechnetate). Additionally, when the amount of stannous chloride dihydrate was increased up to 40 µg per kit, all of three species are found.

All species of technetium in the reaction were determined by thin layer chromatography [31, system of work for $^{99m}Tc$-$MAG_3$]. Comparison between commercial kit with inhouse kit had shown that three components gave the same Rf. value(Table 4.9). This process needs long period to separate free pertechnetate from hydrolyzed reduce technetium and $^{99m}Tc$-$MAG_3$. The novel separation methods were developed and the data were shown in table 4.9. The hydrolysis species was easily separated by ITLC-SG with 85% methanol which was better than ITLC-SG with 0.9% sodium chloride solution. Another species, pertechnetate was not well separated by using common solvent such as acetone. The n-octanol which was recommended solvents to used with ITLC-SG was very slow for the separation and

could not separate all of the three species in one run. The developed method, using whatman paper number I as a media and acetonitrile with variable gradient of aqueous as developing solvent. It was found to be the best system to separate all the species. The data shown that the gradient of water between 20 to 40% could separate three species in this system. The gradient of 65:35 acetonitrile : water was the best condition for the 15 cm separation distant. This condition was used in the following experiment.

Table 4.9 Comparison of Rf value from Reference commercial kit with inhouse kit.

| Species | Reference | | inhouse kit | |
|---|---|---|---|---|
| | Ø.9% NaCl | n-octanol | Ø.9% NaCl | n-octanol |
| RH-Tc | Ø | Ø | Ø | Ø |
| Bound-Tc-$MAG_3$ | 1 | Ø | 1 | Ø |
| Free $TcO_4^-$ | 1 | 1 | 1 | 1 |

Table 4.10 Separation Data of $Tc^{99m}$-$MAG_3$

| Media | solvent | Species | | |
|---|---|---|---|---|
| | | RH-Tc | Bound Tc-$MAG_3$ | Free $TcO_4^-$ |
| ITLC SG | 85% McOH | Ø | 1 | 1 |
| WT No.I | Acetonitrile:$H_2O$ | | | |
| | 50 : 50 | Ø | Ø.7-Ø.9 | 1 |
| | 60 : 40 | Ø | Ø.5-Ø.6 | 1 |
| | 65 : 35 | Ø | Ø.3-Ø.4 | 1 |
| | 70 : 30 | Ø | Ø.Ø-Ø.2 | 1 |
| | 75 : 25 | Ø | Ø.Ø-Ø.1 | 1 |
| | 80 : 20 | Ø | Ø | 1 |
| | 100 : Ø | Ø | Ø | 1 |

## 4.3 A study of Complex formation of $Tc^{99m}$-$MAG_3$ for renal Imaging

The specification of all radiopharmaceuticals for injection should be more than 90% radiochemical purity. The effect of $SnCl_2$ $2H_2O$ quantities, pH and standing time were determined in order to obtain the highest radiochemical purity. The optimum conditions of each factor are described as follow.

The quantities of $SnCl_2.2H_2O$ were varied from 20 µg to 100 µg for reducing Tc(VII) to suitable oxidation state (Tc(V)) for complexing with $MAG_3$ as equation (4)

$$Tc\ (VII) + Sn^{2+} \longrightarrow Tc(V) + Sn^{4++} \qquad (4)$$

Technetium can be reduced to many oxidation states which depends on the strength of reducing reagent. In an aqueous solution, mainly Tc(IV) ($TcO_2.xH_2O$ without chelated) is frequently impurity in the radiopharmaceutical. Technetium chelate and hydrolyzed reduce technetium increased by increasing quantities of stannous chloride dihydrate. While, the pertechnetate ion is decreased. Too much $Sn^{2+}$ will result more hydrolyzed reduce of $^{99m}Tc$ than the complex required. The radiochemical purity of technetium chelate was calculated from radioactivity of $^{99m}Tc$-$MAG_3$ at interested zone divided by total radioactivity of the chromatogram. The hydrolyzed reduce $^{99m}Tc$ and remained free pertechnetate were also determined from their radioactivity divided by the total radioactivity. The figure 4.8 indicates that 50 µg of stannous chloride dihydrate is enough to give more than 90% radiochemical purity. However, 60 µg of stannous chloride dihydrate is selected for future work in order to ensure the complete reduction of pertechnetate ion and prevent hydrolysis species of $TcO_2.xH_2O$ at high quantities of stannous ion.

The redox reaction and chelation depend on the concentration of hydronium ion. The effect of pH, pH 3 to 8 were determined. Radiochemical purity of $^{99m}Tc$-$MAG_3$ in figure 4.9 at low pH shows incomplete reduction and chelation of technetium. When pH increased, chelated technetium is also increased and stabled at pH more than 5. Additionally, from figure 4.11 the species distribution of ligand is shown the hydrolysis species at pH more than 6.5. From this reason, the suitable pH for kit preparation should be performed between pH 5-6.5. Thus pH 5.5 was selected to be stabilized ligand in form of S-Bz-$MAG_3$.

The effect of standing time in Figure 4.10 shows maximum radiochemical purity in 30 minutes after heating in boiling water.Technetium chelated is decreased as indicating by the slope -0.05. The slope of hydrolyzed reduce technetium and free pertechnetate are increased as 0.02 and 0.004 respectively. Therefore, the highest radiochemical purity within 30 minutes should be more than 95%.

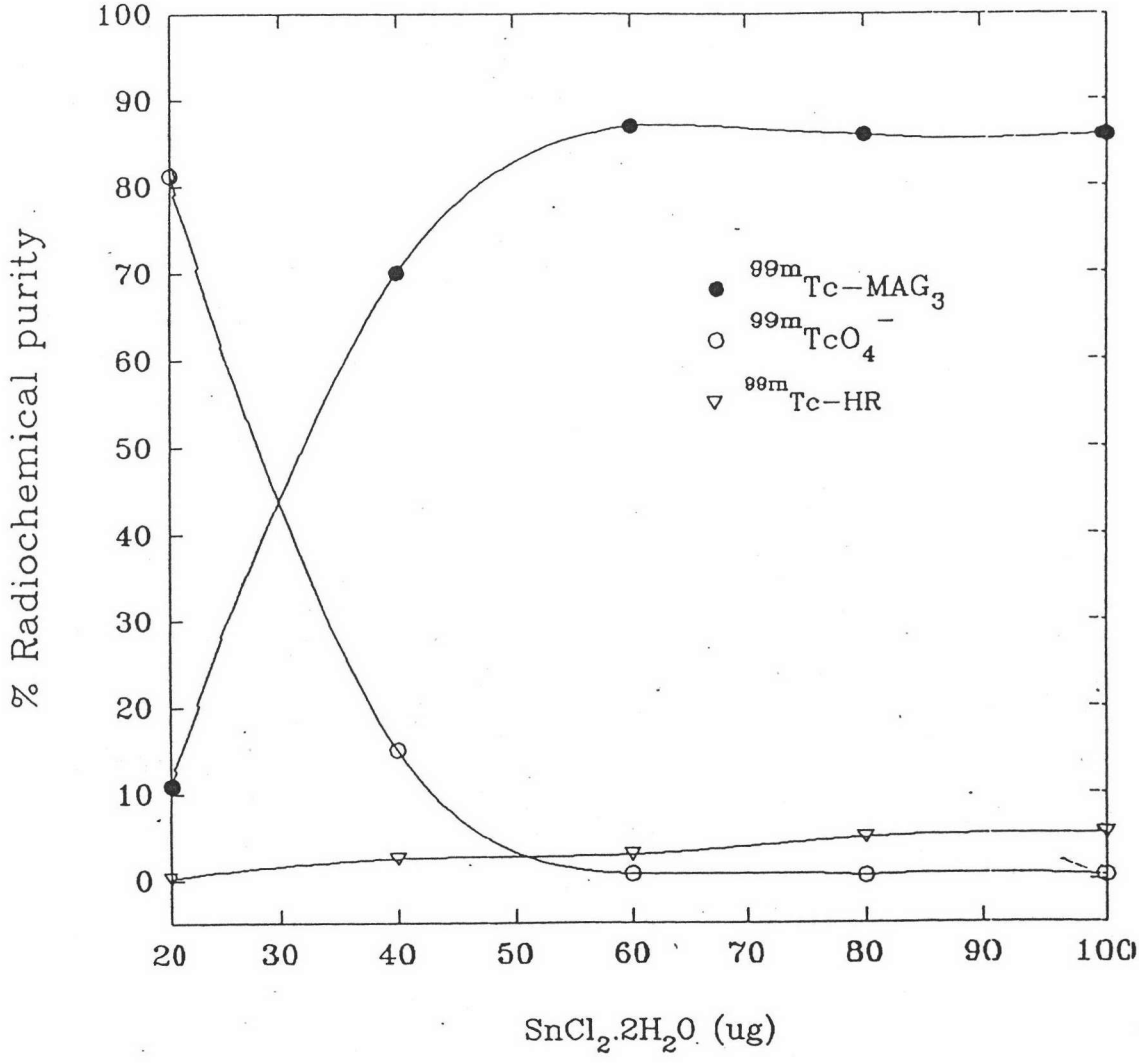


Figure 4.8 Effect of stannous ion on the radiochemical purity of $^{99m}$Tc-MAG$_3$

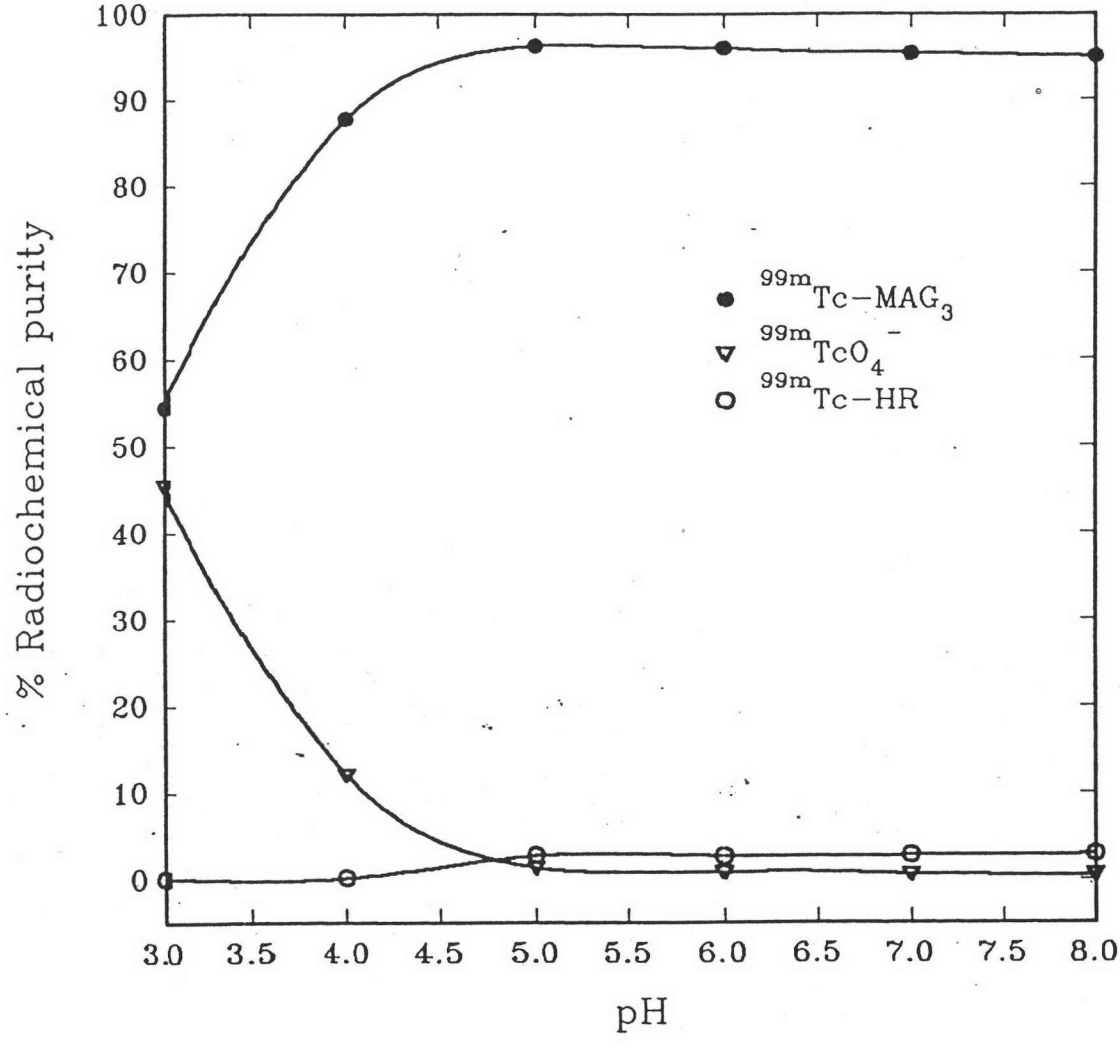


Figure 4.9 Effect of pH on the radiochemical purity of $^{99m}Tc$-$MAG_3$

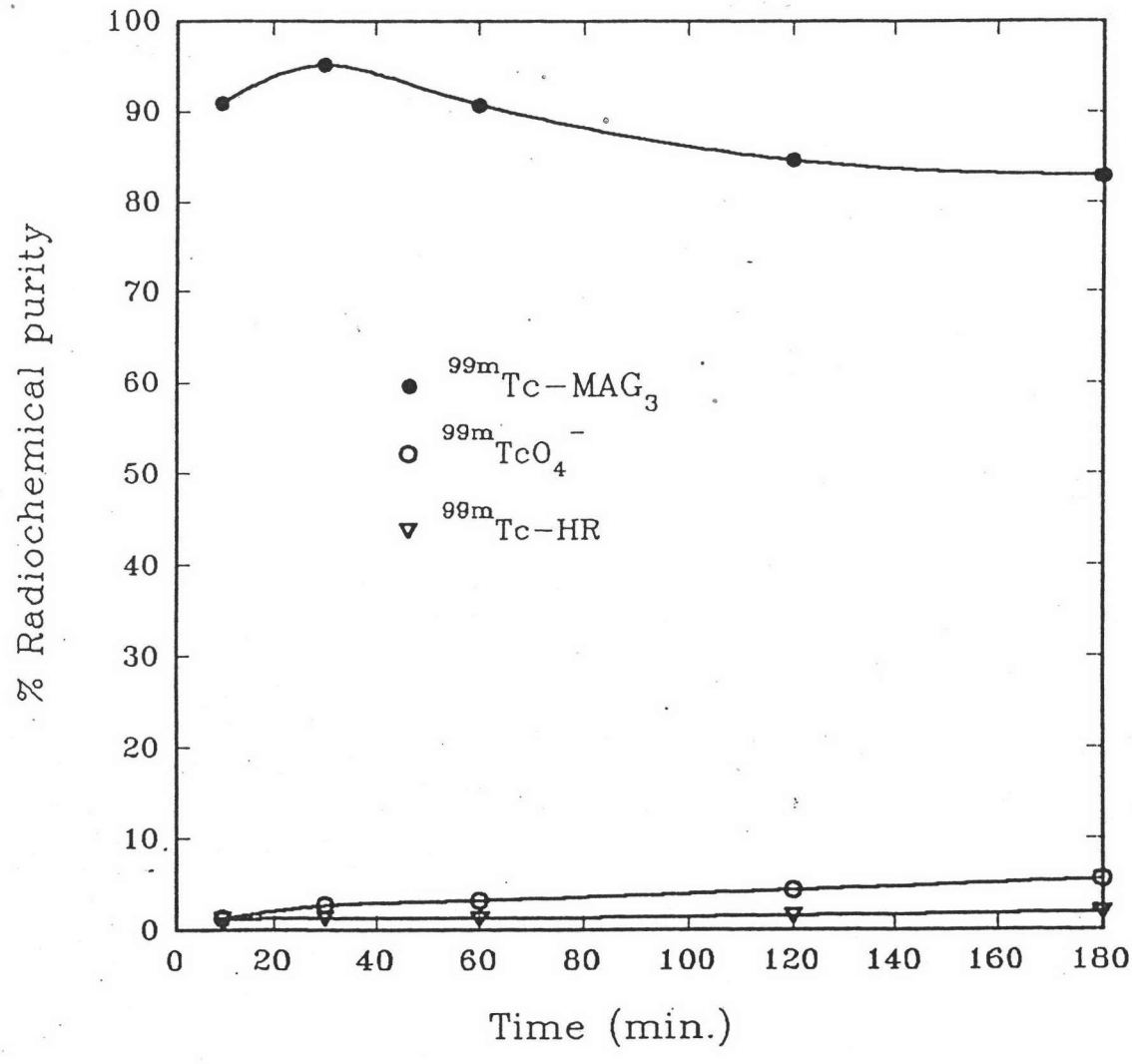


Figure 4.10 Effect of standing time on the radiochemical purity of $^{99m}$Tc-MAG$_3$

## 4.4 Study of Copper(II) complex formation with S-Bz-$MAG_3$

### 4.4.1 Potentiometric and computer calculations

The solution equilibria concerning S-Bz-$MAG_3$ ligand is listed below.

$K_{dimer}$ : $2LH \rightleftharpoons L_2H_2$

$K_a$ : $LH \rightleftharpoons L^- + H^+$

$K_{hydrolysis}$ : $L^- + H_2O \rightleftharpoons L(OH)^{-2} + H^+$

The detected species of S-Bz-$MAG_3$ and with Cu(II) is obtained from the optimizing process by the computer refinement.

Species distribution of S-Bz-$MAG_3$, computed according to the acidity, dimerization and hydrolysis constants,is shown in Figure 4.11. Dimer species of S-Bz-$MAG_3$ ($L_2H_2$) dominates below pH 4.3. The S-Bz-$MAG_3$ or LH species exists below pH 6.Ø. $L^-$ is the major species that survives in the wide pH range (maximum population located within pH range of 5.5 - 8.Ø). $L(OH)^{2-}$ species was found above pH 8.Ø and this species is increased at increasing pH.

The $L(OH)^{2-}$ species corresponding to the hydrolyzed from of S-Bz-$MAG_3$ will finally be decomposed to be the $MAG_3^{2-}$, as the proposed mechanism below.

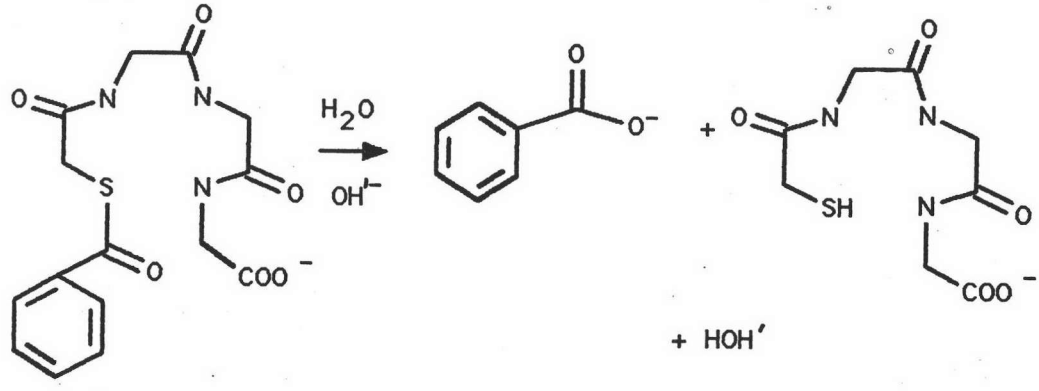


S-Bz-MAG 3 BENZOATE MAG 3

The dissociation constants of the system are shown in Table 4.11. The dissociation constant of ligand is obtained together with the dissociation constant of water ($k_w$), and give a reasonable value of $k_w$ = -13.56.

Table 4.11 The Equilibrium Constants of S-Bz-$MAG_3$

| Constant | Log K |
|---|---|
| $K_{dimer}$ | 2.12 ± 0.05 |
| $K_a$ | -3.47 ± 0.01 |
| $K_{hydrolysis}$ | 3.34 ± 0.02 |

The formation constant of S-Bz-$MAG_3$ with copper(II) ion corresponds to the equation as following.

$$M^{+2} + L^{-} + 2H_2O \rightleftharpoons [ML(OH)_2]^{-1} + 2H^{+}$$

$$M^{+2} + L^{-} + 4H_2O \rightleftharpoons [ML(OH)_4]^{-3} + 4H^{+}$$

The species distribution of the complex obtained from the computer refinement shown in Figure 4.12. The distribution of $[ML(OH)_2]^{-1}$ and $[ML(OH)_4]^{-3}$ are dominated at pH 8 and pH over than 10 respectively. The formation constant of these complexes are shown in table 4.12

Table 4.12 The stability constants of Cu(II) complexes

| Formation Equation | Log K |
|---|---|
| $M+L^{-}+2H_2O \quad [ML(OH)_2]^{-1}+2H^{+}$ | $K_{ML(OH)} = 18.71\pm0.11$ |
| $M+L^{-}+4H_2O \quad [ML(OH)_4]^{-3}+4H^{+}$ | $K_{ML(OH)} = 26.68\pm0.16$ |

The first species, $[ML(OH)_2]^{-1}$ was hydrolysis species. This species should be hydrolyzed at thioester position. The formation constant is closely related to the formation of metal ion in the range of organic and inorganic catalyzing reaction [31-33]. This important class of reaction includes catalyzing equation of transition metal complexes and catalyzing hydrolysis of such organic compound as ester and peptides.

Metal ion can act equally well as catalysts for hydrolysis of ester of organic acid, for instance in the $M^{2+}$ catalysis of hydrolysis of ester such as $M^{2+}$ with thio-oxalate [34]. $Cu^{2+}$ is more effective than $H^{+}$, in breaking the ester linkage . This hydrolysis of ester is catalyzed by Cu(II) ions in order to activate some appropriate point in the organic molecule should induce nucleophilic attaction by water or hydroxide ion [35]. For this species, the hydrolysis of ester was found to be more rapid than deprotonation of amine. From ligand titration, it can obtain only one hydrolysis species, which should be hydrolysis of benzoyl group, because at this pH the external base cannot deprotonize the nonchelated amine.

The second species, $[ML(OH)_4]^{-3}$ should be deprotonated of three amide from triglycine in $MAG_3$. The deprotonize at amide was similar to copper(II) triglycine and copper(II) tetraglycine complex(11). Routes involving cleving of hydrogen from the $\alpha$ atom of the precursor are an important entry to metal-ligand. The majority of such reactions are most easily understood as deprotonation reaction. However, case that are represented better as a transfer of hydrogen atom (e.g. eq 1) are also known [36].

$$\begin{array}{c} X \\ | \\ M-QH_2 \\ | \\ X \end{array} \xrightarrow[HX]{-HX} \begin{array}{c} X \\ | \\ M=QH \end{array} \xrightarrow[HX]{-HX} M\equiv Q \qquad (1)$$

The position of this equilibrium will depend on these conditions : I) raising the oxidation state of metal II) use of strongly basic leaving groups (X) III) addition of an external base to consume HX or IV) increasing the steric congestion around metal.

The oxidation state of metal enhances the acidity of coordinated group($-NH_2$, $NH_3$, $H_2O$, etc). At the same time it empties d-orbital for π-donation. According to this reason, the deprotonation of $NH_2$-group in $MAG_3$ can be occurred similarly as in sulfonamide, since the negative charge can disperse over the copper(II) ion plus oxygen from peptide bond instead of over just one oxygen plus nitrogen[37]. For this reason, both species $[ML(OH)_2]^{-1}$, $[ML(OH)_4]^{-3}$ were represented as complexes of $[CuMAG_3(OH)]^{-1}$ and $[CuMAG_3]^{-3}$ respectively. The proposed structures of these complexes are shown in Figure 4.11. The species distribution is plotted in Figure 4.13.

(A)

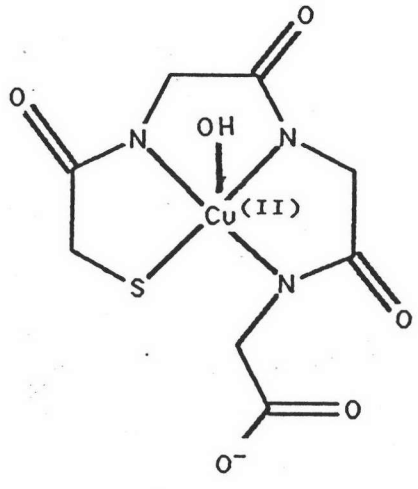


$[CuMAG_3(OH)]^{-1}$

(B)

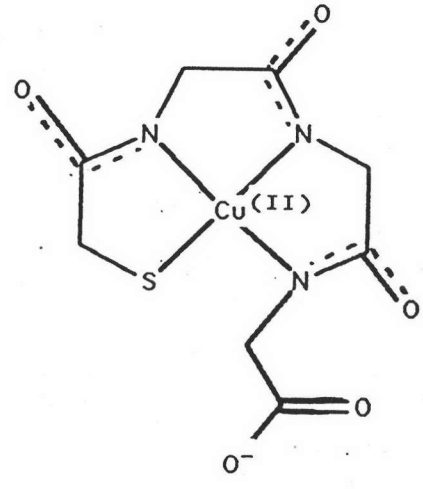


$[CuMAG_3]^{-3}$

Figure 4.11 Propose structure of Cu(II) with $MAG_3$

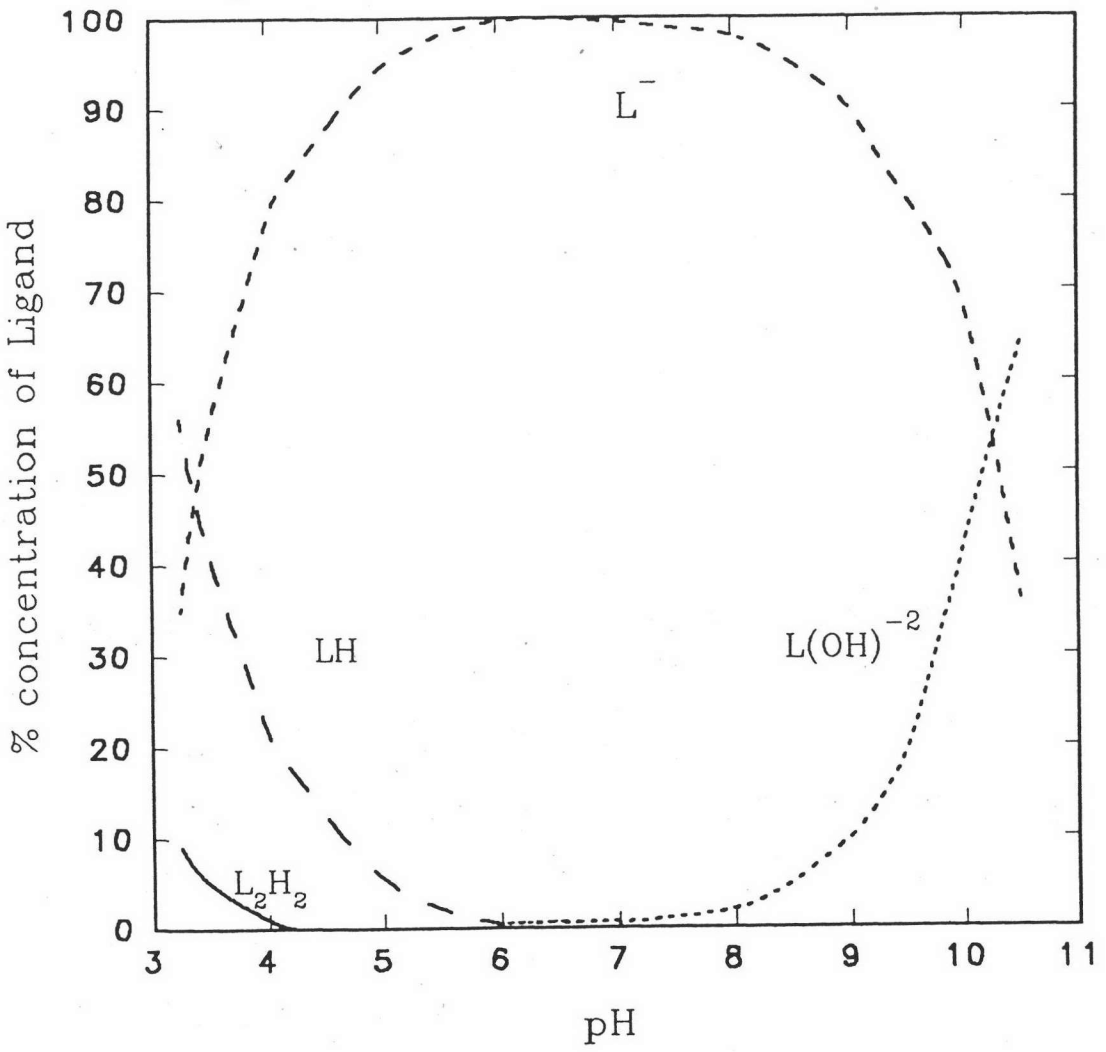


Figure 4.12 The species distribution of S-Bz-$MAG_3$. These curves were plotted using calculated data from SUPERQUAD program, based on ligand concentration is 1.2 mM.

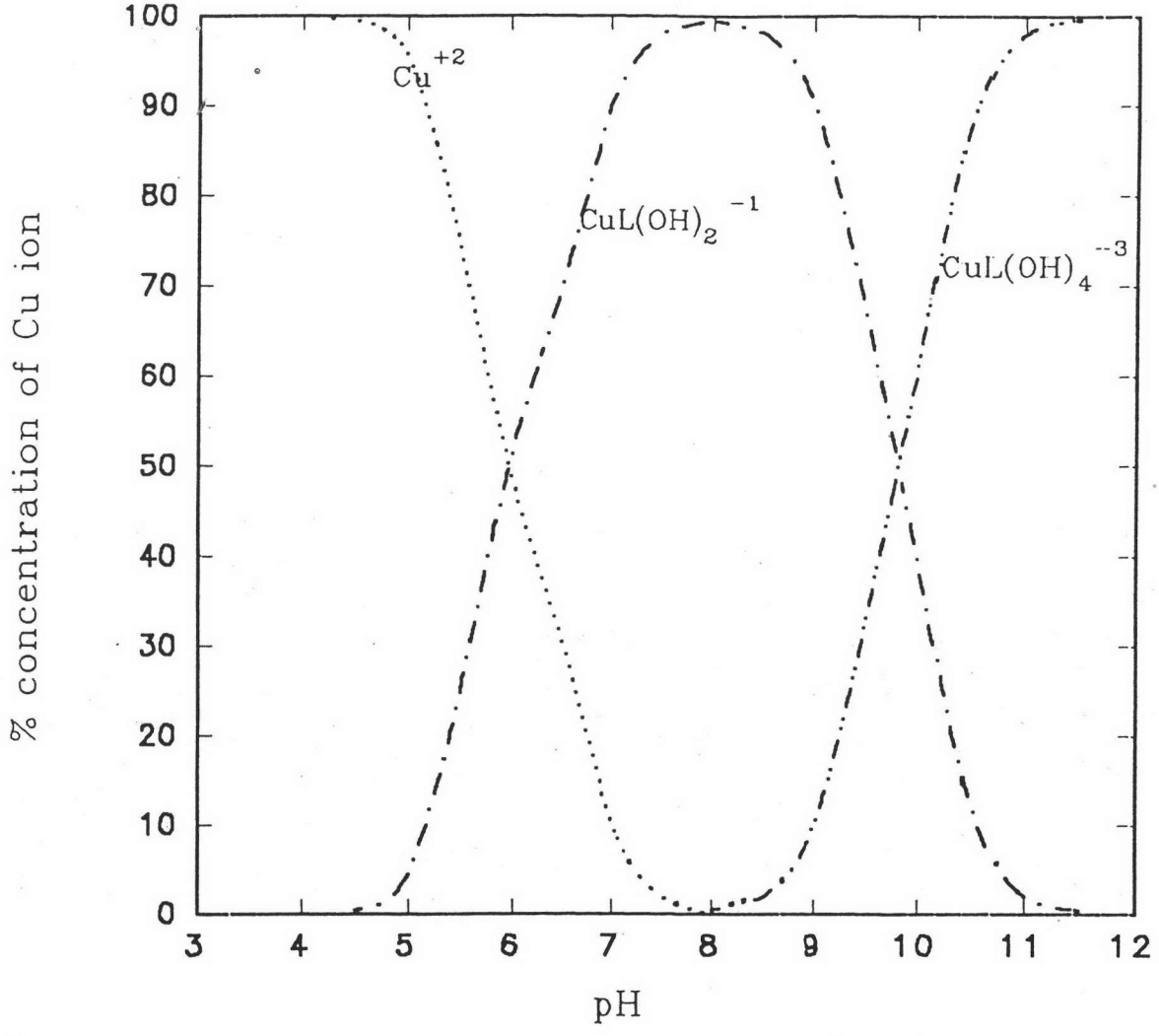


Figure 4.13 the species distribution of Cu(II)-$MAG_3$. These curves were plotted using calculated data from SUPERQUAD program, based on metal and ligand concentration are 0.99 mM and 1.98 mM respectively.

4.4.2 Stoichiometric and the Apparent stability constant study of complex by UV/vis spectroscopy

The measurement of the $[CuMAG_3(OH)]^{-1}$ and $[CuMAG_3]^{3-}$ spectrum were carried out at pH 8 and over 12 respectively. The spectrum of the first complex shown two peakes at 270 nm and 635 nm, which are the same as those of the reactant. The spectrum is shown in figure 4.14. Stoichiometry of the first complex cannot be determined by spectroscopy method. It's should be assumed from the second complex because the model from computer refinement gave the same ratio of metal and ligand.

The second complex of Cu(II) with $MAG_3$ was confirmed by UV/visible spectroscopy. The spectra shown three peaks at 250, 310 and 494 nm. Mole ratio, mole fraction and slope ratio can be employed in stoichiometric study. The selected wavelength for this complex was 494 nm, as shown in Figure 4.13. Its was clearly seen in Figure 4.14, 4.15, and 4.16. That $MAG_3$ is bound to $Cu^{+2}$ ion in the ratio of 1:1 complex.

The results from potentiometric titration and UV/visible spectroscopy indicated that there might be the effect of Cu(II) in $^{99m}Tc$-$MAG_3$ complex, either combination of Cu(II) with $^{99m}Tc$-$MAG_3$ complex or competition to $MAG_3$ in complexing with Tc. This effect can also be confirmed by the radiochemical purity of $^{99m}Tc$-$MAG_3$ in the presence of various amount of Cu(II), as shown in 4.19

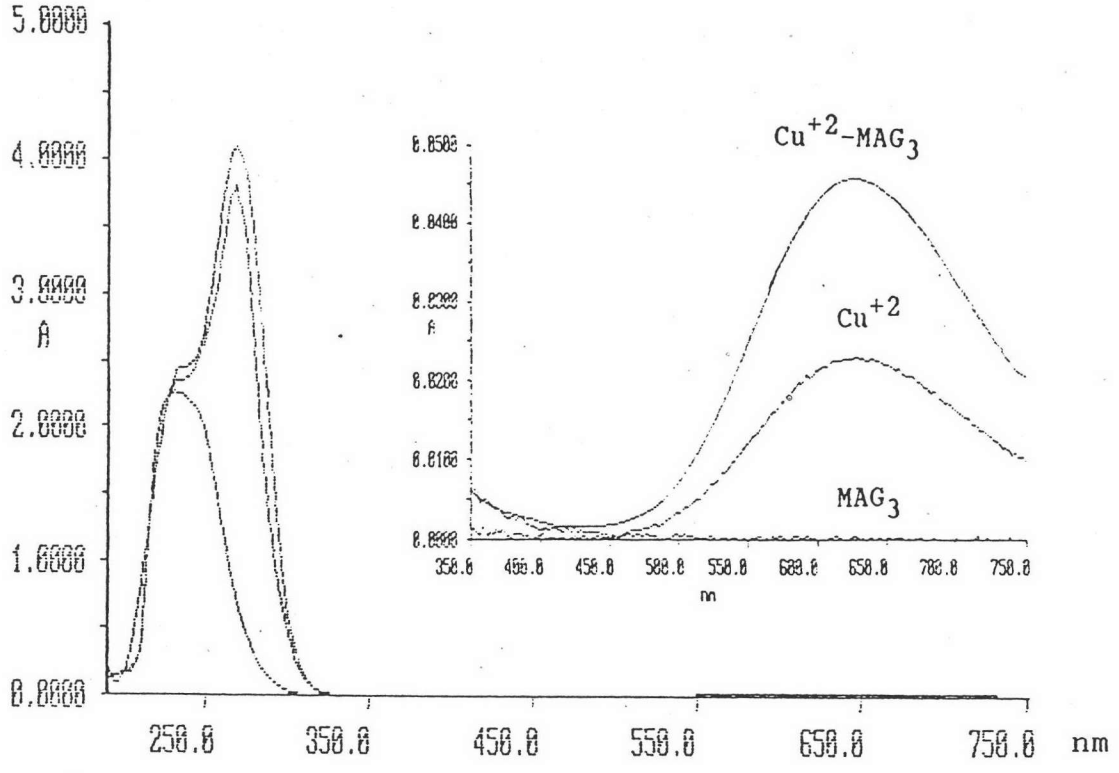


A) The UV/vis spectra of Cu-$MAG_3$ complex compare with its reactant.

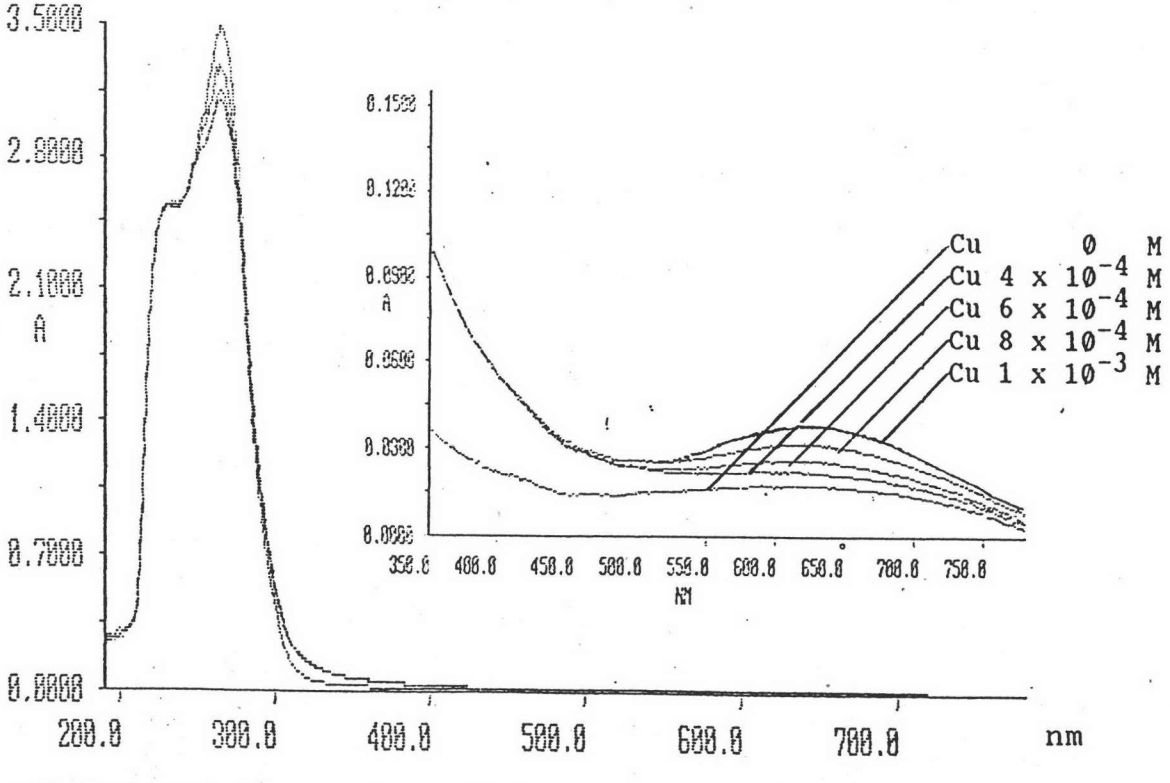


B) The UV/vis spectra of Cu-$MAG_3$ at Cu(II) concentration from 0 to 1 x $10^{-3}$ M

Figure 4.14 The optimum absorption of Cu(II)$MAG_3$ at pH 8

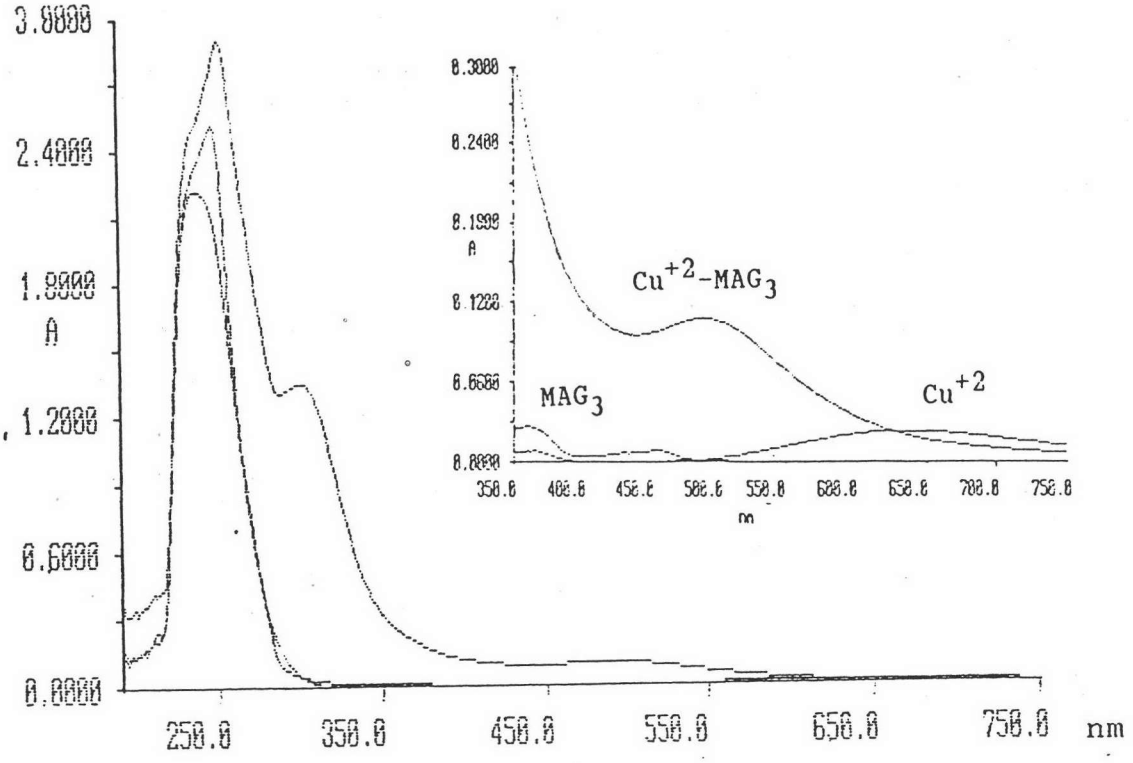


A) The UV/vis spectra of Cu-$MAG_3$ complex compare with its reactant.

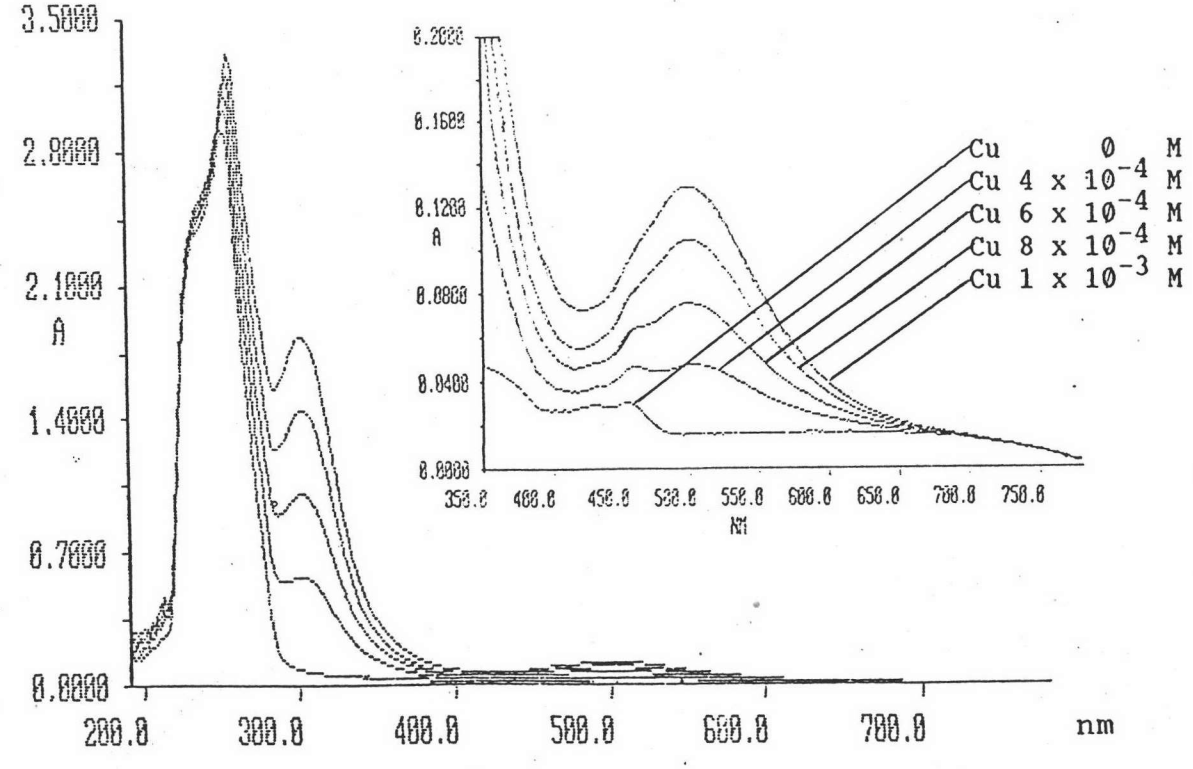


B) The UV/vis spectra of Cu-$MAG_3$ at Cu(II) concentration from 0 to 1 x $10^{-3}$ M

Figure 4.15 The optimum absorption of Cu(II)$MAG_3$ at pH 12

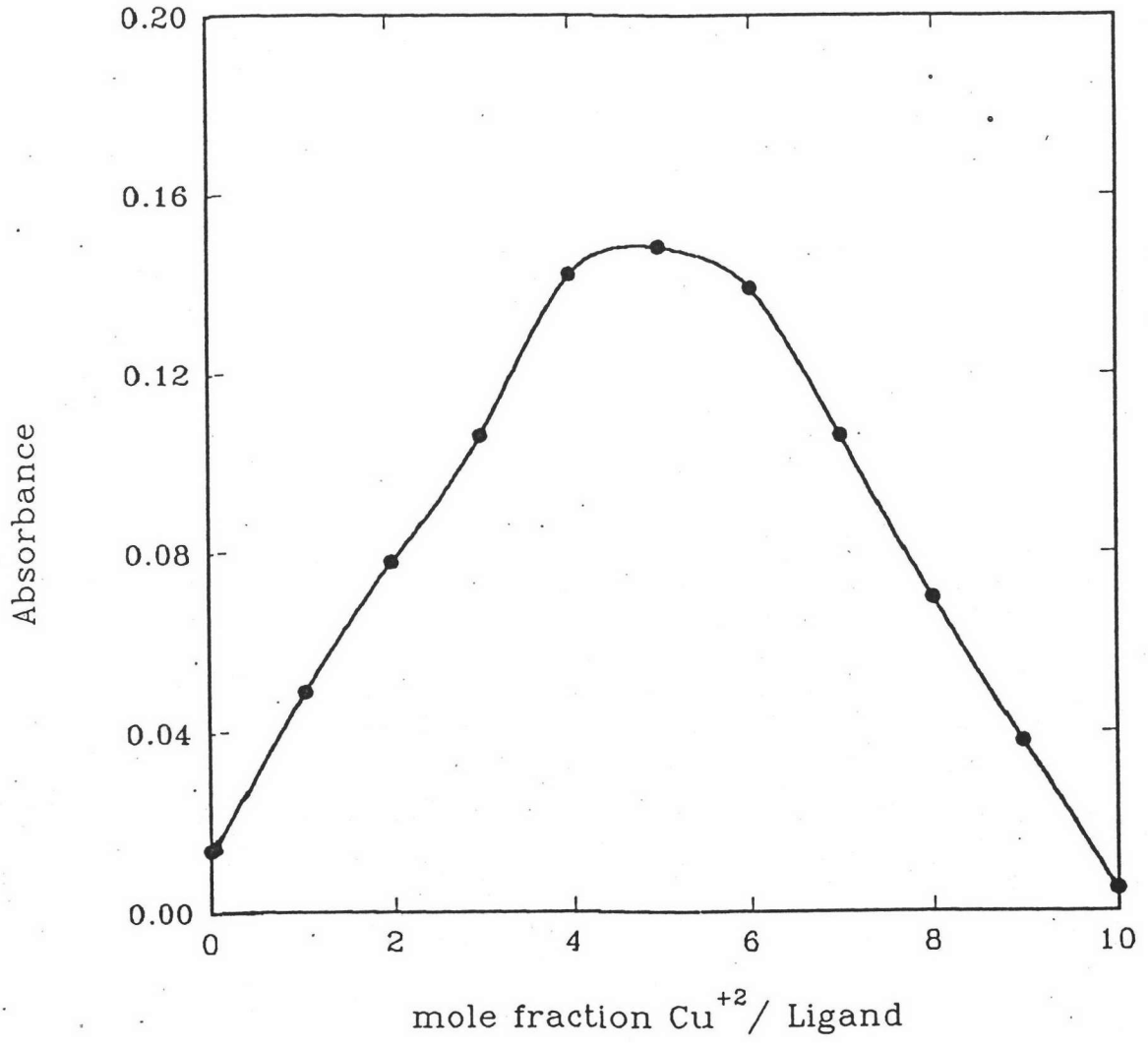


Figure 4.16 The Job's method plot of Cu(II)-$MAG_3$ at 494 nm

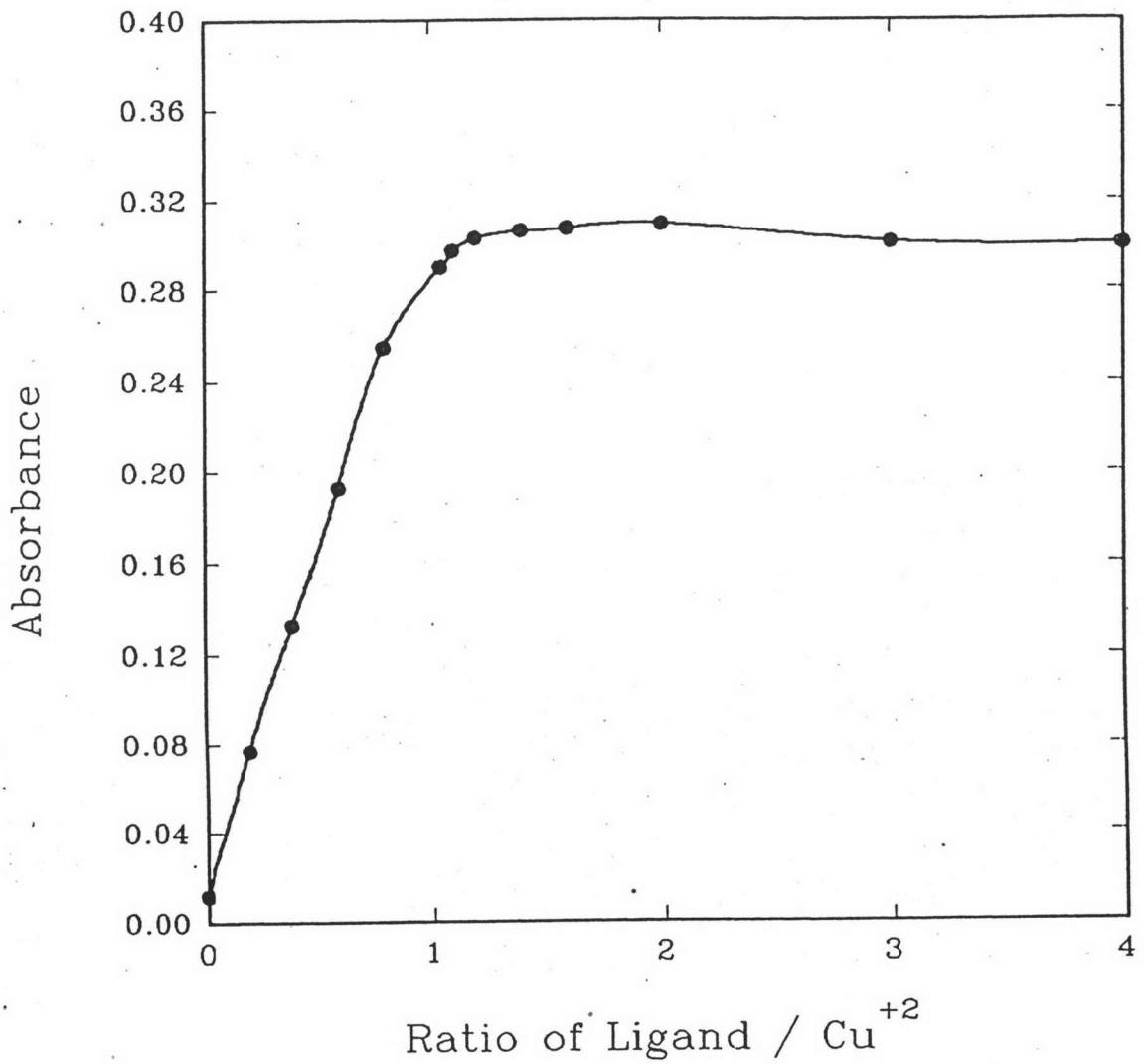


Figure 4.17 The mole ratio plot of Cu(II)-$MAG_3$ at 494 nm

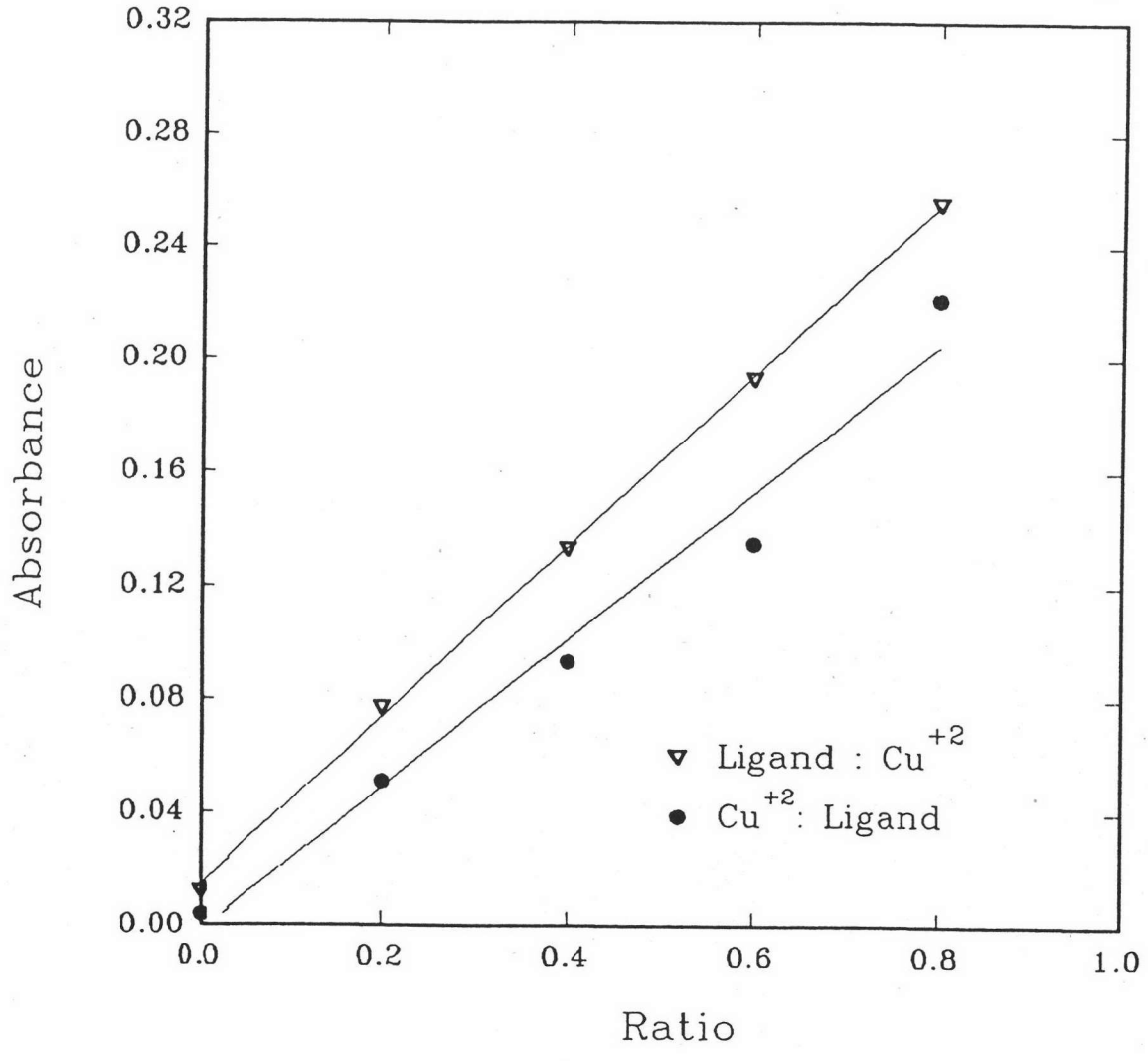


Figure 4.18 The plots of slope ratio at 494 nm. The slope of Ligand : $Cu^{+2}$ and $Cu^{+2}$ : Ligand are Ø.Ø51 and Ø.Ø49 respectively. The ratio of Cu : Ligand is closely to 1:1

## 4.5 Influence of Cu(II) on $^{99m}$Tc-MAG$_3$

In the presence of Copper(II) ion in $^{99m}$Tc-MAG$_3$, the radiochemical purity of $^{99m}$Tc-MAG$_3$ was decreased, depending on the quantities of Cu(II) ion and standing time. For the period of 10 to 180 minutes and the quantities of Cu(II) ion from 0 to 900 µg, the decreasing slope of $^{99m}$Tc-MAG$_3$ are tabulated in table 4.13. The maximum quantity of Cu(II) was equal to the loosely bound copper in normal human plasma. This data indicates that Copper(II) can reduce the radiochemical purity of $^{99m}$Tc-MAG$_3$. Plotted of radiochemical purity are shown in figure 4.19.

Table 4.13 The decreasing slope of radiochemical purity of $Tc^{99m}$-MAG$_3$, by Cu(II)

| Cu(II) (µg) | slope |
|---|---|
| 0.00 | -0.055 |
| 90.00 | -0.055 |
| 225.00 | -0.061 |
| 445.00 | -0.082 |
| 675.00 | -0.096 |
| 900.00 | -0.110 |

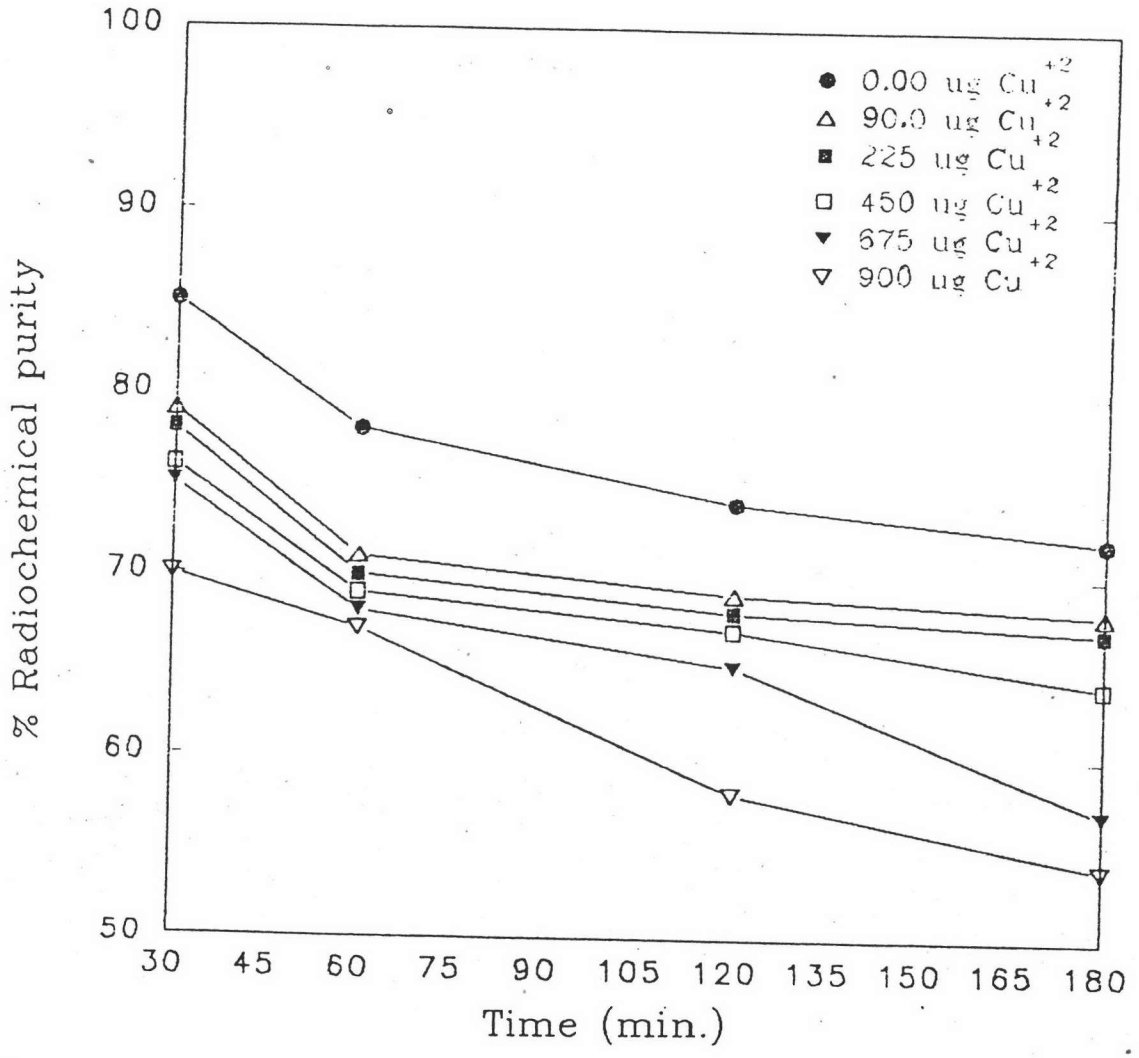


Figure 4.19 Influence of Cu(II) on radiochemical purity of $^{99m}Tc\text{-}MAG_3$